# Precise Electromagnetic Tests of *Ab Initio* Calculations of Light Nuclei: States in $^{10}$Be

E. A. McCutchan,[1] C. J. Lister,[1] R. B. Wiringa,[1] Steven C. Pieper,[1] D. Seweryniak,[1] J. P. Greene,[1] M. P. Carpenter,[1] C. J. Chiara,[1,2] R. V. F. Janssens,[1] T. L. Khoo,[1] T. Lauritsen,[1] I. Stefanescu,[2] and S. Zhu[1]

[1]*Physics Division, Argonne National Laboratory, Argonne, Illinois 60439, USA*

[2]*Department of Chemistry and Biochemistry, University of Maryland, College Park, Maryland 20742, USA*

(Received 6 July 2009; revised manuscript received 7 October 2009; published 4 November 2009)

In order to test *ab initio* calculations of light nuclei, we have remeasured lifetimes in $^{10}$Be using the Doppler shift attenuation method (DSAM) following the $^{7}$Li($^{7}$Li, $\alpha$)$^{10}$Be reaction at 8 and 10 MeV. The new experiments significantly reduce systematic uncertainties in the DSAM technique. The $J^\pi = 2_1^+$ state at 3.37 MeV has $\tau = 205 \pm (5)_{\rm stat} \pm (7)_{\rm sys}$ fs corresponding to a $B(E2\downarrow)$ of $9.2(3)e^2$ fm$^4$ in broad agreement with many calculations. The $J^\pi = 2_2^+$ state at 5.96 MeV was found to have a $B(E2\downarrow)$ of $0.11(2)e^2$ fm$^4$ and provides a more discriminating test of nuclear models. New Green's function Monte Carlo calculations for these states and transitions with a number of Hamiltonians are also reported and compared to experiment.

DOI: 10.1103/PhysRevLett.103.192501 PACS numbers: 21.10.−k, 21.60.De, 23.20.−g, 27.20.+n

Our understanding of nuclei is being reshaped by new ''first principles'' calculations based on realistic interactions between nucleons. They encompass a fundamental goal of nuclear structure studies: the understanding of how nuclear properties emerge from the basic forces. Several *ab initio* approaches which start from ''bare'' nucleon-nucleon ($NN$) potentials (that reproduce elastic $NN$ scattering data) and empirical three-nucleon ($3N$) potentials are now being developed. Most applicable to light nuclei are the Green's function Monte Carlo (GFMC) [1,2] method and the no-core shell model (NCSM) [3,4]. These methods have been successful in reproducing many features, including binding energies and excitation spectra [5], charge radii [6,7], and electromagnetic moments [8]. One important aspect emerging from these calculations is the essential requirement of a $3N$ force, providing new insight into the origin of the spin-orbit force, decoupling of poorly bound neutrons, and clustering of nucleons in light nuclei. Since the parametrization of the $3N$ force is still under development, high-quality measurements in light nuclei are now timely. In this Letter, we report on new experiments to precisely measure lifetimes of bound states in $^{10}$Be. New GFMC calculations with a number of realistic forces which explore the sensitivity to $3N$ potentials are also presented.

The $A = 10$ nuclei have long provided a stringent test of nuclear models. Kurath [9] discussed the need for an unusually strong spin-orbit interaction to correctly reproduce the sequence of levels in $^{10}$B. In these nuclei, the $p$ shell is half-filled and more than one state can be created with the same spin-parity $J^\pi$, isospin $T$, and spatial symmetry. For example, in the LS shell model basis, $^{10}$Be has two $J^\pi = 2^+$, $T = 1$, $^1D[442]$ states at 3.37 and 5.96 MeV. These states have very different properties and provide a delicate test of both the Hamiltonians and the calculational methods. The Argonne $v_{18}$ (AV18) $NN$ [10] interaction predicts a separation of only 0.23(15) MeV for these states, one with a negative (*oblate*) intrinsic quadrupole moment and a small $B(E2)$ decay to the ground state, and one with a positive (*prolate*) quadrupole moment which is much more collective. The oblate state is lower in energy with just AV18. Calculations including $3N$ potentials tend to separate the states and bring the more collective prolate level lower in energy. The ratio of electromagnetic decays from these states to the ground state is extremely sensitive to structure and varies from 4:1 to >50:1 in different models.

The states of interest have short lifetimes, a few to hundreds of femtoseconds, so Coulomb excitation and the Doppler shift attenuation method (DSAM) are appropriate experimental techniques for measuring these lifetimes. The study of $^{10}$Be following $\beta n$ decay of $^{11}$Li was recently shown to also be very powerful for this specific case [11,12]. We have concentrated on inferring lifetimes using DSAM which relies on establishing the initial velocity of nuclei in the state of interest and then measuring the mean velocity at decay after decelerating in a slowing material. From this velocity difference, the level lifetime can be determined if the slowing history of the ion is known. To provide significant constraints on the new calculations a precision better than <5% in the $E2$ matrix elements is needed, which is considerably more stringent than normally required for testing nuclear models. To move beyond the >25% measurements from the 1960s [13,14], we have developed an improved DSAM which focuses on reducing many of the systematic uncertainties. Careful selection of the kinematic conditions and control of feeding from higher lying levels are critical. These refinements, coupled with making the measurements at high velocities where stopping powers are best characterized, and advancements in $\gamma$-ray detection, yield a much improved DSAM which can dramatically reduce uncertainty in the lifetime measurements.

Excited states in $^{10}$Be were populated in the $^{7}$Li($^{7}$Li, $\alpha$)$^{10}$Be reaction. $^{7}$Li beams of up to 50 pnA and

 

energies of 8 and 10 MeV were produced by the ATLAS accelerator and impinged on thin $^{7}$Li metal and $^{7}$LiF targets. Target backings of copper and gold of sufficient thickness to slow the recoiling nuclei to about half their original energy were used. Gamma rays from the reaction were detected with Gammasphere [15], consisting of 100 Compton-suppressed HPGe detectors in 16 azimuthally symmetric rings mounted from $\theta = 32°$ to 163° to the beam direction. The efficiency of the array (10% for 1-MeV $\gamma$ rays) and its granularity allowed many systematic tests to be made. Upon exiting the target, the nuclei recoiling along the beam direction were then detected in the Argonne fragment mass analyzer (FMA) [16] positioned 90 cm downstream of the target and subtending $1° \times 2°$. The FMA rejected most noninteracting beam particles ($>10^{8}$ suppression) and transported $^{10}$Be ions with charge state $q = 3^{+}$ to the focal plane. Selection of a particular $q$ creates a small bias in recoil velocity selection; in the present case this is significantly smaller than the uncertainty in the measured mean velocity. The transmitted ions were identified 50 cm behind the focal plane in a 20 cm deep, two-electrode ionization chamber operated at 15–30 torr.

Knowledge of the stopping power of the slowing material is essential for extracting a lifetime from DSAM. At low energies, the nuclear component of the stopping contributes significantly, giving uncertainties in the predicted stopping power and recoil direction. At sufficiently high energies, the stopping becomes 99.99% electronic which is well known and understood. To reduce systematic errors in stopping powers, we chose a reaction with a high positive $Q$ value ($Q = +11.4$ MeV) resulting in $^{10}$Be nuclei with high initial recoil energy, ~15 MeV. This is in contrast to previous experiments [13,14] where the recoil energy was <1 MeV. Since in the present technique, the recoils must exit the backing layer with sufficient velocity to be detected at the focal plane of the FMA, the measurement is made over a limited velocity range, $\beta = v/c = 4$–6%. This is ideal for DSAM as only a small portion of the Bragg curve is sampled in the region where stopping is best known. This is also in contrast to traditional DSAM where recoils are usually stopped in the backing layer and thus span the velocity range from initial velocity to $\beta = 0$. The characterization of Li and Be ions slowing in Li, LiF, Cu, and Au were taken from the SRIM package [17], which parametrizes the vast body of stopping data now available.

Another key component in DSAM is knowing the angle between the recoiling nuclei and the $\gamma$-ray emission. In traditional DSAM, scattering in the backing material produces a distribution of recoil velocity vectors which have to be modeled in the analysis. Use of the FMA to select a single recoil velocity vector (only the $^{10}$Be nuclei traveling at 0° to the beam axis) provides a significant improvement to DSAM. Furthermore, due to the simple two-body kinematics of the reaction used in the present work, the initial recoil speed along the beam direction is well defined. An additional benefit of using the FMA is that direct population of states can be selected, thereby eliminating cascade feeding. In a plot of $\Delta E$ vs $E_{\mathrm{tot}}$ for the ionization chamber, given in Fig. 1, three distinct recoil groups are observed corresponding to direct population of the ground state (group 1), the $2_1^+$ state (group 2), and the set of four states around 6 MeV (group 3). The wide strip below the $^{10}$Be recoils corresponds to $^{7}$Li scattered beam. Gating on the direct population of the $2_1^+$ state (group 2), an exceptionally clean spectrum with a single $\gamma$ ray is observed (Fig. 1, top panel). Selection of the lower energy recoils (group 3) gives the decay of the ~6 MeV states (Fig. 1, middle panel).

For each state there is an optimum target layering, depending on the lifetime. For maximum sensitivity, equal numbers of decays should occur in the target production layer, in the slowing medium, and in the post-target flight region. Care was taken to monitor the thicknesses of targets and backings, using both weighing and $\alpha$ gauging, before and after the experiments, as this is a key source of systematic uncertainty. Several target materials and backings were used to investigate systematic effects. Lithium metal targets with thickness of 100–200 $\mu$g/cm$^2$ were produced in an evaporator and transferred to the Gammasphere cham-

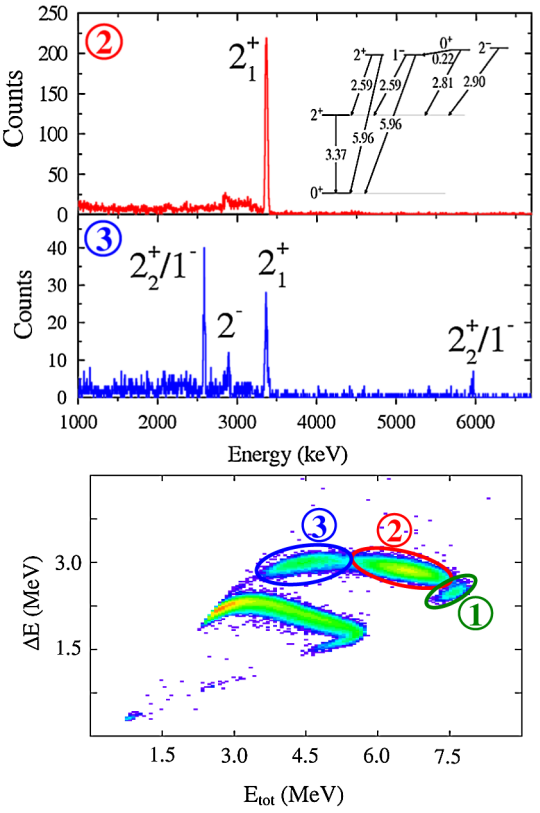


FIG. 1 (color online). (Top and middle) Spectra gated on $^{10}$Be recoil groups with the $\gamma$-ray transitions labeled by the decaying state. (Bottom) Energy loss versus total energy from the ionization chamber behind the focal plane of the FMA. The circled regions correspond to direct population of distinct $^{10}$Be levels. The top panel inset shows a level scheme for the five bound excited states in $^{10}$Be with $\gamma$-ray energies in MeV.

ber in a vacuum interlock [18] maintained at $<10^{-5}$ torr. LiF targets were also used to provide a contrasting stopping power in the target layer.

The lifetime of the first excited state of $^{10}$Be was determined by measuring the centroid of the 3.37-MeV, $2_1^+ \rightarrow 0_1^+$ transition as a function of detector angle. The $\gamma$ ray (Fig. 1 panel 2) was measured in each of the 16 angle groups in Gammasphere. The measured centroid as a function of $\cos(\theta)$ for a Cu backing is given in Fig. 2(a), compared to a fit using the relativistic Doppler shift formula. Centroids were measured with sufficient precision that higher-order terms quadratic in $\cos(\theta)$ were clear, and small mechanical misalignments could be corrected for. The quality of the fit is more clearly illustrated in Fig. 2(b). Here, the measured centroids are divided by the best fit function, $\sqrt{1-\beta^2}/(1-\beta\cos(\theta))$ with $\beta = 0.05109$. Although the mean velocity of nuclei at the time of $\gamma$-ray emission produced in each target-backing combination varied widely, they all led to consistent lifetimes. The mean lifetimes extracted from the analysis of the different backings are summarized in Table I. The calculation of the velocity-lifetime relationship was made by subdividing both the production target and backing into 30 layers and determining the average velocity profile and the probability of emission in each layer. The inferred lifetime did not change when a finer layering was used. Both the statistical uncertainties (from the fit to the Doppler shifts) and the systematic uncertainties (from thickness and stopping power) varied considerably for the different target-backing arrangements. However, the many varied measurements allowed appraisal of systematic uncertainties.

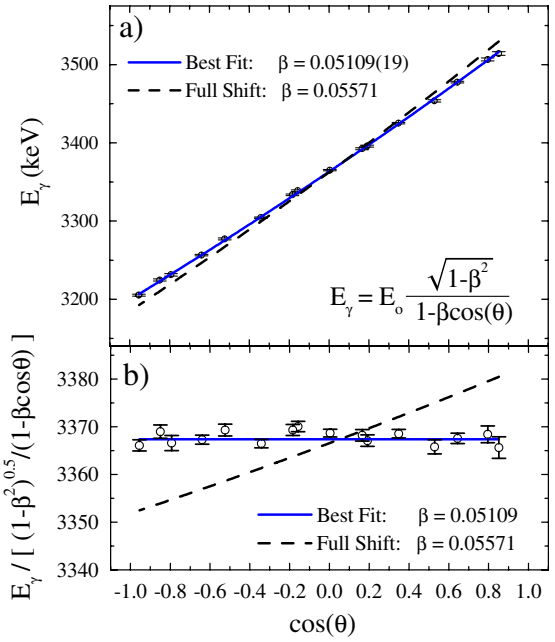


FIG. 2 (color online). (a) Measured centroid of the 3.37-MeV transition for each of the Gammasphere angle groups compared to a fit with the relativistic Doppler formula (solid line) and to the maximum velocity (dashed line). (b) Similar to (a) but normalized to the best fit function with $\beta = 0.051\,09(19)$.

The 3.37-MeV level was measured in nine separate experiments. The weighted mean value is $\tau = 205 \pm (5)_{\text{stat}} \pm (7)_{\text{syst}}$ fs which gives a reduced transition probability $B(E2\downarrow) = 9.2(3)e^2$ fm$^4$. Our lifetime is about 10% longer than the mean of previous experiments [19] which span the range 110 to 260 fs at the $1\sigma$ level. The leading contribution to systematic uncertainty was the target layer thickness, especially for the lithium metal targets. The next leading term was the uncertainty in the stopping power of the slowing medium, which is now at the $<2.5\%$ level for this velocity regime [17].

The four bound states near 6 MeV were all populated and spectroscopic information was extracted. For this discussion, we focus on the second $J^\pi = 2^+$ state at 5.96 MeV. This level is part of a close-lying doublet with a $J^\pi = 1^-$ level that is only $\sim$1.5 keV higher and the $\gamma$ decays from the two states could not be resolved. Thus, analysis of the 2.59-MeV and 5.96-MeV transitions yielded different "effective" lifetimes of 50(8) and 30(8) fs, respectively, highlighting the doublet nature of the transitions. Unfolding the doublets required knowledge of the $\gamma$-branching ratios from each level and their relative population intensities. Combining these two quantities and the measured "effective" lifetimes, the second $2^+$ state was found to have $\tau = 59 \pm (15)$ fs. For the $2_2^+ \rightarrow 0_1^+$ branch, we used the precise value of 6.1(1)% measured in neutron capture [20]. In the decay to the ground state, this gives $B(E2\downarrow) = 0.11(2)e^2$ fm$^4$. Complete details of the analysis will be given in a future paper [21].

In parallel to the experimental work, extensive GFMC calculations of states and transitions in $^{10}$Be were carried out using AV18 and a variety of 3$N$ forces, see Table II. The absolute GFMC energies are believed to be accurate to 1%–2%, with somewhat larger errors for the excitation differences. The GFMC method for evaluating transition strengths is detailed in Ref. [8]. Calculations with AV18 alone predict near degeneracy for the two $J^\pi = 2^+$ states, with the oblate state slightly lower in energy. To explore the sensitivity to 3$N$ potentials, calculations were performed with AV18 plus Urbana-IX (UIX), Illinois-2

TABLE I. Mean lifetimes from different target and backing combinations determined for the 3.37-MeV level in $^{10}$Be.

| Target ($\mu$g/cm$^2$) | Backing (mg/cm$^2$) | $\tau$ (fs) | $\Delta\tau_{\text{stat}}$ (fs) |
|---|---|---|---|
| 208 $^7$Li | 3.00 Cu | 203 | $\pm 9$ |
| 208 $^7$Li | 2.66 Cu | 209 | $\pm 13$ |
| 266 $^7$LiF | 2.28 Cu | 200 | $\pm 23$ |
| 208 $^7$Li | 2.07 Cu | 189 | $+29-26$ |
| 266 $^7$LiF | 2.16 Cu | 204 | $+46-37$ |
| 90 $^7$Li | 2.69 Cu | 208 | $\pm 17$ |
| 120 $^7$Li | 2.33 Au | 223 | $+67-60$ |
| 266 $^7$LiF | 2.16 Cu | 203 | $\pm 13$ |
| 214 $^7$LiF | 0.99 Cu | 217 | $+63-40$ |

TABLE II. GFMC calculations of the $^{10}$Be ground-state, $E_{gs}$, and excitation, $E_x$, energies (both in MeV), and $B(E2\downarrow)$ transitions in $e^2$ fm$^4$ compared to experimental values. The numbers in parentheses for the calculations are Monte Carlo statistical errors. Calculations were done with a variety of potentials to explore the sensitivity in predicting electromagnetic matrix elements.

| $H$ | AV18 | AV18 + UIX | AV18 + IL2 | AV18 + IL7 | Exp. |
|---|---|---|---|---|---|
| $\lvert E_{gs}(0^+)\rvert$ | 50.1(2) | 59.5(3) | 66.4(4) | 64.3(2) | 64.98 |
| $E_x(2_1^+)$ | 2.9(2) | 3.5(3) | 5.0(4) | 3.8(2) | 3.37 |
| $E_x(2_2^+)$ | 2.7(2) | 3.8(3) | 5.8(4) | 5.5(2) | 5.96 |
| $B(E2; 2_1^+ \rightarrow 0^+)$ | 10.5(3) | 17.9(5) | 8.1(3) | 8.8(2) | 9.2(3) |
| $B(E2; 2_2^+ \rightarrow 0^+)$ | 3.3(2) | 0.35(5) | 3.3(2) | 1.7(1) | 0.11(2) |
| $\Sigma B(E2)$ | 13.8(4) | 18.2(6) | 11.4(4) | 10.5(3) | 9.3(3) |

(IL2), and Illinois-7 (IL7) [22]. Inclusion of the 3$N$ forces lifts the degeneracy between the $2^+$ states, slightly for UIX, more so for IL2, and approaching the experimental spacing with the IL7 potential.

Similar trends were found for the $B(E2)$ strengths to the ground state. With just AV18, the calculations overpredict both transition strengths. UIX provides a good description of the decay of the $2_2^+$ state, yet significantly overpredicts the decay of the $2_1^+$ state. With the IL potentials, it appears that, as the $2^+$ states become farther apart in energy, the predicted $B(E2\downarrow)$ strengths tend to approach the experimental values. Considering both the energies and transition strengths, the IL7 potential provides the best description. The first excited $2^+$ state decay is now well reproduced but there is too much strength calculated for the second $2^+$ state decay. This shortcoming is still being investigated. It could possibly be remedied by further refinement of the Illinois 3$N$ potentials, or by including more extended $2^+$ components arising from particles promoted into the next (sd) shell model orbits.

A wide variety of other models have also been used to investigate $^{10}$Be. In the traditional $p$ shell model with unmixed $K$-quantum number, Millener [23] predicts $B(E2; 2_1^+ \rightarrow 0_1^+) = 11.8e^2$ fm$^4$ and the ratio of $B(E2)$s as 50:1. Both the NCSM with the CD-BONN, $NN$ potential [3] and the microscopic cluster model (MCM) [24] tend to underpredict the $B(E2; 2_1^+ \rightarrow 0_1^+)$ value, with NCSM predicting $6.6e^2$ fm$^4$ and the MCM predicting $6.1e^2$ fm$^4$. However, both predict a weak $B(E2; 2_2^+ \rightarrow 0_1^+)$ transition strength, $\sim 0.13e^2$ fm$^4$, in good agreement with experiment. Reconciling the results from GFMC, NCSM, and cluster models is an interesting and ongoing process.

In conclusion, the Doppler shift attenuation method (DSAM) has been refined to precisely determine the lifetime of the first excited $J^\pi = 2^+$ state in $^{10}$Be. Care was taken to control the systematic uncertainties usually associated with DSAM. High-precision lifetime measurements now appear feasible in not only light nuclei, but also a range of systems which can be produced through two-body kinematic reactions. The lifetime of the $2_2^+$ state in $^{10}$Be was also measured. New *ab initio* calculations show the sensitivity of the transition matrix elements to nuclear structure, especially to the form of 3$N$ forces.

This work was supported by the DOE Office of Nuclear Physics under Contract No. DE-AC02-06CH11357, DE-FG02-94ER40834, and under SciDAC Grant No. DE-FC02-07ER41457. Calculations were performed on the SiCortex computer of the Argonne Mathematics and Computer Science Division.

[1] Steven C. Pieper, K. Varga, and R. B. Wiringa, Phys. Rev. C **66**, 044310 (2002).
[2] Steven C. Pieper and R. B. Wiringa, Annu. Rev. Nucl. Part. Sci. **51**, 53 (2001).
[3] E. Caurier, P. Navrátil, W. E. Ormand, and J. P. Vary, Phys. Rev. C **66**, 024314 (2002).
[4] P. Navrátil and W. E. Ormand, Phys. Rev. C **68**, 034305 (2003).
[5] Steven C. Pieper, Nucl. Phys. **A751**, 516 (2005).
[6] P. Mueller *et al.*, Phys. Rev. Lett. **99**, 252501 (2007).
[7] W. Nörtershäuser *et al.*, Phys. Rev. Lett. **102**, 062503 (2009).
[8] Muslema Pervin, Steven C. Pieper, and R. B. Wiringa, Phys. Rev. C **76**, 064319 (2007).
[9] D. Kurath, Phys. Rev. **101**, 216 (1956); **106**, 975 (1957).
[10] R. B. Wiringa, V. J. G. Stocks, and R. Schiavilla, Phys. Rev. C **51**, 38 (1995).
[11] H. O. U. Fynbo *et al.*, Nucl. Phys. **A736**, 39 (2004).
[12] C. M. Mattoon *et al.*, Phys. Rev. C **80**, 034318 (2009).
[13] E. K. Warburton *et al.*, Phys. Rev. **148**, 1072 (1966).
[14] T. R. Fisher, S. S. Hanna, D. C. Healey, and P. Paul, Phys. Rev. **176**, 1130 (1968).
[15] I. Y. Lee, Nucl. Phys. **A520**, c641 (1990).
[16] C. N. Davids *et al.*, Nucl. Instrum. Methods Phys. Res., Sect. B **70**, 358 (1992).
[17] J. F. Ziegler, J. P. Biersack, and M. D. Ziegler, *SRIM: The Stopping of Ions in Matter* (Lulu Press, Morrisville, NC, 2008), http://www.srim.org.
[18] E. A. McCutchan, C. J. Lister, and J. P. Greene, Nucl. Instrum. Methods Phys. Res., Sect. A **607**, 564 (2009).
[19] D. R. Tiley *et al.*, Nucl. Phys. **A745**, 155 (2004).
[20] T. J. Kennett, W. V. Prestwich, and J. S. Tsai, Nucl. Instrum. Methods Phys. Res., Sect. A **249**, 366 (1986).
[21] E. A. McCutchan *et al.* (to be published).
[22] B. S. Pudliner *et al.*, Phys. Rev. Lett. **74**, 4396 (1995); S. C. Pieper *et al.*, Phys. Rev. C **64**, 014001 (2001); S. C. Pieper, AIP Conf. Proc. **1011**, 143 (2008).
[23] D. J. Millener, Nucl. Phys. **A693**, 394 (2001); (private communication).
[24] Jim Al-Khalili and Korji Arai, Phys. Rev. C **74**, 034312 (2006).